Using syntectonic remagnetizations for fold geometry and vertical axis rotation: the example of the Cévennes border (France)

Bernard Henry,[1] Henri Rouvier[1,2] and Maxime Le Goff[1]

[1]*Géomagnétisme et Paléomagnétisme, IPGP and CNRS,* 4 *avenue de Neptune,* 94107 *Saint-Maur cedex, France. E-mail: henry@ipgp.jussieu.fr*
[2]*Laboratoire de Géologie Appliquée, Paris VI University,* 4 *place Jussieu,* 75252 *Paris cedex* 05, *France*

SUMMARY

Classical progressive unfolding makes a distinction between pre-folding, post-folding or synfolding magnetization. It yields the direction of magnetization only in the two first cases. To determine the direction of synfolding magnetization, possible different unfolding percentages during remagnetization have to be assumed according to the site. The small circle approach of Surmont *et al.* not only leads to this direction, but also to the dip value at each site during remagnetization. In the Cévennes area, extensive palaeomagnetic study reveals syntectonic remagnetization enabling the reconstruction of the shape of a fold for the time of the magnetic overprinting as well as analysis of the rotations undergone by some sites after the remagnetization.

Key words: bootstrap, fold, remagnetization, rotation, syntectonic.

INTRODUCTION

Within deformed areas, rock can acquire 'syntectonic' remagnetization between the beginning of the first deformation and the end of the last one (i.e. possibly between two tectonic phases, contrary to what geologists would consider one syntectonic event). If the fold axes during the different tectonic events have similar orientations, the direction of this remagnetization can be determined. With this aim in view, simple progressive unfolding is generally applied and the retained direction is that corresponding to the unfolding percentage associated with the optimal value of correlation or scattering parameters based on the magnetization directions (McElhinny 1964; McFadden & Jones 1981; McFadden 1990; Fisher & Hall 1990, 1991; Bazhenov & Shipunov 1991; Tauxe *et al.* 1991; Watson & Enkin 1993; Tauxe & Watson 1994; Enkin & Watson 1996). However, such an approach is mostly biased because, at each stage of folding, the percentage of existing deformation relative to final deformation is not always the same at the different sites. The aim of this paper is to determine the initial orientation of syntectonic magnetic overprint independently of the mean unfolding percentage and to obtain structural information from the orientation of the remagnetization.

In this paper, we make a distinction between applications to structural deformations with folding with the axis close to the horizontal (called here 'folds') and with rotations with the axis close to the vertical (called here 'rotations'). It is obvious that if the actual axis is known this axis has to be used for the fold and rotation corrections (Henry 1983).

DETERMINATION OF THE DIRECTION OF A SYNTECTONIC REMAGNETIZATION

McClelland-Brown (1983), Surmont *et al.* (1991) and Shipunov (1997) used the fact that, during tilting, the direction of magnetization moves on the projection sphere along a small circle. Intersection of the circles from different sites represents the single possible common magnetization direction during the whole deformation, and therefore the remagnetization direction. Such a method cannot be used when the fold axis has the same orientation at all the sites (either no circle intersections or total overlapping of the circles). In this case, the direction of the syntectonic remagnetization cannot be determined at all within a small circle, even if a classical progressive unfolding yields an optimal unfolding percentage with perfect clustering of the magnetization directions. In fact, we then know the relative position of the limbs of the fold but not their position relative to the horizontal plane.

To determine the best intersection of small circles, the least-squares method is applied. This means that the palaeomagnetic direction retained on each small circle is that closest to the best intersection. The improvement of the clustering of the palaeomagnetic data occurring during unfolding can be then estimated by the decrease in size and ellipticity (Henry & Le Goff 1994; Henry *et al.* 1999; Derder *et al.* 2001) of the confidence region of the palaeomagnetic direction. This can be accomplished by comparing these confidence regions before dip correction, at optimal unfolding obtained by the small circles method and after dip correction. We have,
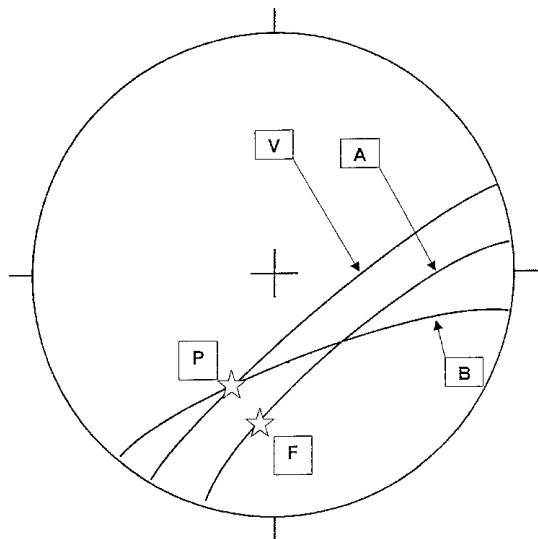
Figure 1. Effect on the orientation of a small circle of an error (circle A) related to the choice of a wrong palaeomagnetic direction (star F) or (circle B) on the dip declination. The true small circle (V) and palaeomagnetic direction (star P) are shown. Stereographic projection in the lower hemisphere.

however, to keep in mind that this improvement is often overestimated because the small circle approach is an optimization technique. The clever projection (all points of the sphere projected orthogonally onto the projection plane) of Shipunov (1997) unfortunately does not retain the angles, and thus the least-squares results, determined in the projection plane, are mostly partly biased. The iterative method (McFadden & McElhinny 1988) used by Surmont *et al.* (1991) remains the best. However, the reliability of the results obtained using small circles is not always the same for three reasons:

(1) When all circles are almost parallel, a small variation in the orientation of the circles can change the intersection direction significantly (Fig. 1). Thus it seems clear that the intersection direction has to be associated with a confidence region to be reliable.

(2) When each circle corresponds to the mean magnetization direction derived from several samples with the same dip in one site, each circle has the same weight for the determination of the intersection, whatever the number of samples and the precision parameter associated with the magnetization direction. Thus this confidence region must integrate the uncertainty on each palaeomagnetic direction.

(3) As for most of the dip corrections, the small circles method does not take into account the uncertainty on dip measurement. Dip azimuth has, however, a major effect on small circle orientation (Fig. 1). For low absolute values of dip plunge, the uncertainty on dip azimuth is often very important. In an overturned geological unit, this could create major bias in determining the direction of remagnetization. The confidence region from the small circles approach has therefore to take into account the uncertainty on dip determination.

The bootstrap method (Efron 1982; Efron & Tibshirani 1986) has already been used to determine the confidence region (Constable & Tauxe 1990; Tauxe *et al.* 1991; Henry 1997a,b, 1999). If *n* mean data A are obtained by *n* bootstrapping of data B, the maximum density contour including 95 per cent of these *n* mean data A is the confidence region at 95 per cent. Use of this contour instead of the calculated equivalent elliptical confidence region enables several

possible confidence subregions to be identified, thus pointing out non-homogeneity of the data B. A minimum number of data points is necessary for the application of the bootstrap method. The results are definitely significant for more than 15 samples (Efron & Tibshirani 1986), and 10 samples would seem to represent the minimum number of samples. The results are clearly not statistically significant for fewer than seven samples (too low a number of possible different resamplings). If each B value is associated with an uncertainty window, bootstrap also allows this uncertainty to be taken into account (for example for a bootstrap based on mean site palaeomagnetic direction B from different sites, the confidence region is the α_{95} for each site). Tauxe & Watson (1994) proposed to use the parametric bootstrap: at each resampling, the B values are obtained by randomly sampling within the uncertainty window. If the uncertainty window corresponds to a particular distribution (for example the Fisher distribution) (Fisher 1953), the sampling can be made on a large data set created to have the same uncertainty windows with the same distribution. If the values B have been determined from a sufficient number of measured data C (for example, for a site, mean palaeomagnetic direction B from samples with palaeomagnetic directions C), it is possible is to use another bootstrap of the C data to obtain the B data at each resampling.

For determination of the confidence region at 95 per cent of syntectonic remagnetization, bootstrap enables the best intersection of the small circles to be determined. The latter include either the magnetization direction of each sample or the mean magnetization direction for all samples with the same dip in each site. In this last case for each site, at each resampling, the mean direction can be obtained by another bootstrap using the direction obtained from the samples (if the number of samples is sufficient). Another possibility is to use direction by site randomly chosen within the α_{95} uncertainty window (the Fisher parametric bootstrap, Tauxe & Watson 1994).

In the field, dip value mostly corresponds to the mean of numerous dip measurements obtained in the same area. It is then possible to use these measurement values for another bootstrap at each resampling. Another possibility is to estimate the uncertainty on the dip in each site; a parametric bootstrap (Tauxe & Watson 1994) is then made within the uncertainty window (uniform distribution) on the dip (Table 1).

Fig. 2 presents an example of determination of the remagnetization direction with its confidence region. Small circles B are based on mean site data. They have been obtained using the mean palaeomagnetic direction for the site from bootstrap of the samples' palaeomagnetic data C. For the dip, parametric bootstrap has been used for an uncertainty of 5° on the dip azimuth.

DETERMINATION OF THE DIP DURING REMAGNETIZATION

The best intersection of small circles corresponds on each circle to different partial dip correction. The dip value used for this partial correction is that existing at the site during the acquisition of remagnetization. It can be associated with a confidence region determined during the bootstrap calculation of the best intersection of the small circles. One palaeomagnetic direction corresponds to each bootstrapped best intersection on each small circle and thus to one corresponding dip value (i.e. one corresponding stratification pole). This allows, for each site, *n* stratification poles from which can be determined the maximum density contour which includes 95 per cent of these *n* poles. The dip value at each site, with its uncertainty

Table 1. Determination of the remagnetization direction.

C			B				A
Dip in the site	→	Bootstrap	↘				
			Each small circle at each resampling	→	Bootstrap	→	Remagnetization direction with confidence region
Palaeomagnetic directions in the site	→	Bootstrap if mean site direction is used for small circle	↗				
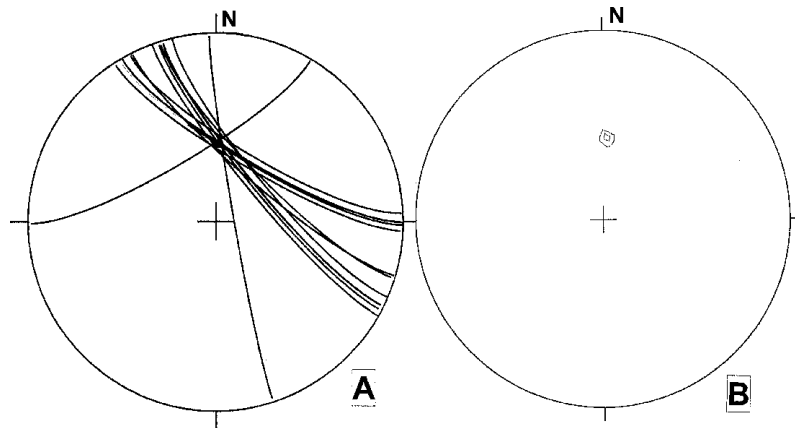
Figure 2. Small circles (A) and confidence regions at 95 per cent and 63 per cent (B) associated with the syntectonic remagnetization determined by Henry *et al.* (2001) and Rouvier *et al.* (2001) on the Cévennes border. Stereographic projection in the lower hemisphere.

(determined from the stratification pole confidence region) is then obtained for the time of remagnetization and could then be used for structural applications (see for example Stamatakos & Hirt 1994; Jordanova *et al.* 2001).

Lewchuk *et al.* (2002) studied syntectonic remagnetization in two sections of a large fold (at Medley and Rig in the Patterson Creek anticline) in the Appalachian Mountains (southern Virginia). Details about the geological setting and palaeomagnetic data are given by Lewchuk *et al.* (2002). This fold is mainly simple, with minor deformations relative to a perfect regular case and with an almost horizontal fold axis. There is, therefore, no evidence of superimposed folding having a fold axis with a significantly different orientation. Simple progressive unfolding leads to slightly different remagnetization directions in two formations of the stratigraphic series. However, there is nothing to indicate several remagnetization events and this difference is related to the application of simple progressive unfolding. Fig. 3(a) shows the small circles corresponding to data of Lewchuk *et al.* (2002) and Fig. 3(b) the best intersection with its associated confidence region obtained by bootstrap. For the bootstrap, we applied here an uncertainty of 5° on the azimuth of dip direction. This confidence region is relatively small at Rig, but larger at Medley: thus the remagnetization direction is not very well specified. The precise dip therefore cannot then be determined at each site.

However, the remagnetization direction was the same at all the sites during magnetic overprinting. Only one dip value for each site corresponds to any direction of remagnetization within the confidence region (Fig. 3b). The uncertainty windows concerning the dip from different sites are then not independent, and any dip value for a site within this window corresponds to only one dip value in the uncertainty window for each of the other sites. The interesting information is that the relative difference in dip between two sites is almost independent of the chosen common direction of re-

magnetization within its confidence region. It is therefore possible to determine the shape of the fold but not its precise position relative to the horizontal. Figs 4(a) and (b) represent, in the two cross-sections, the shape of the same fold, for the same bed (presented here assuming that the remagnetization direction corresponds to the best intersection of the small circles). Only one site of Lewchuk *et al.* (2002) has not been considered because of very large uncertainty about its mean palaeomagnetic direction. Because the present dip is considered here only in the different studied sites (and not in all the locations of the fold), it is possible that the calculated present shape of the fold (the dip between two sites has been chosen as the mean of the dip in these sites) does not perfectly correspond to its actual shape in the field. This presents no problem in our analysis because our main aim is to compare this 'calculated' present shape (Fig. 4a) with the calculated shape during remagnetization (Fig. 4b) in the same sites. To illustrate part of the folding occurring after remagnetization, Fig. 4(c) shows the present deformation of a plane, which should have been horizontal during remagnetization. At Medley, the shape of the fold during remagnetization appears very simple and asymmetrical, with a large monoclinal structure towards the northwest and a small steeper limb in the southeast. The fold axis after remagnetization migrates northwestwards, and the folding becomes almost symmetrical, with a sharp hinge. At Rig, during remagnetization, the structure is a little more complicated, with a second small fold axis in the northwestern part. After remagnetization, the fold has a much more regular curvature than at Medley. In both sections, most of the folding occurred after remagnetization.

APPLICATIONS TO THE CÉVENNES BORDER

A palaeomagnetic study has been carried out in sedimentary rocks from Carboniferous to Jurassic ages in the Cévennes border (Fig. 5)
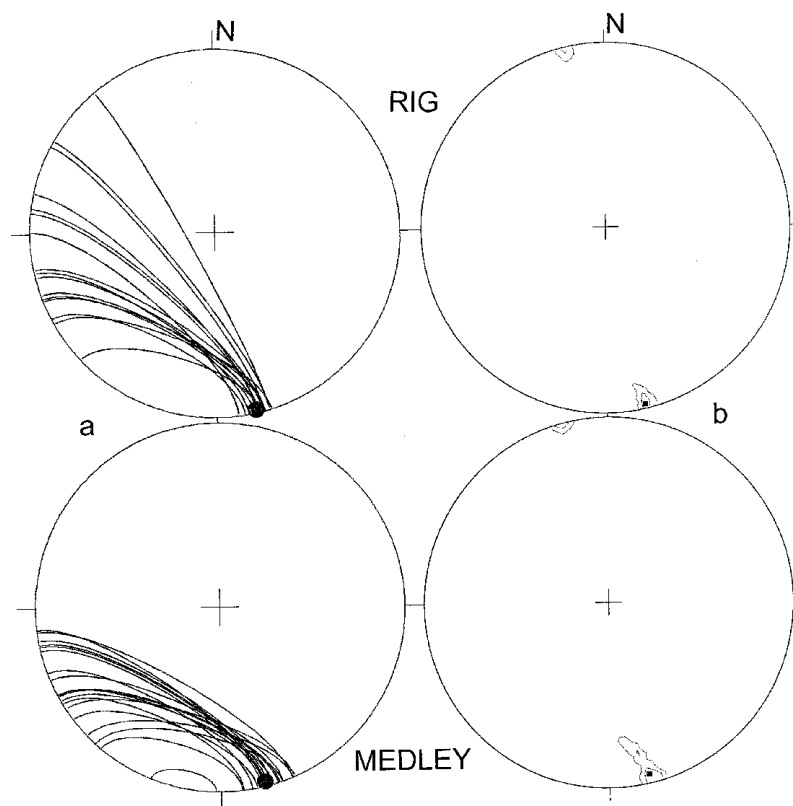
Figure 3. Small circles (a) and confidence regions at 95 per cent and 63 per cent (b) associated with the syntectonic remagnetization on the Appalachian Mountains fold at Medley and at Rig (Lewchuk *et al.* 2002). Stereographic projection in the lower hemisphere.
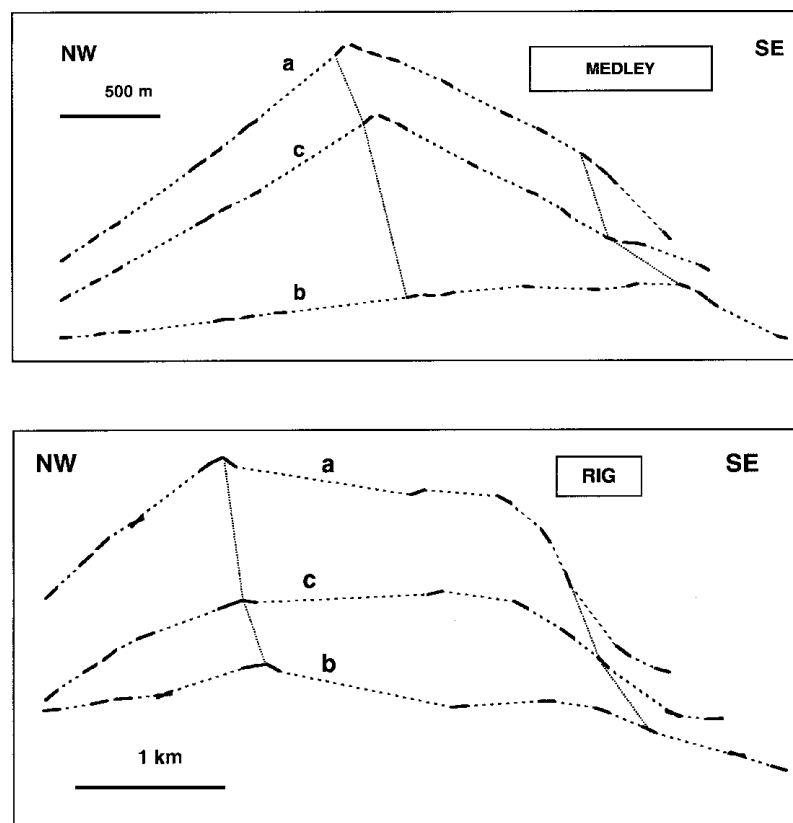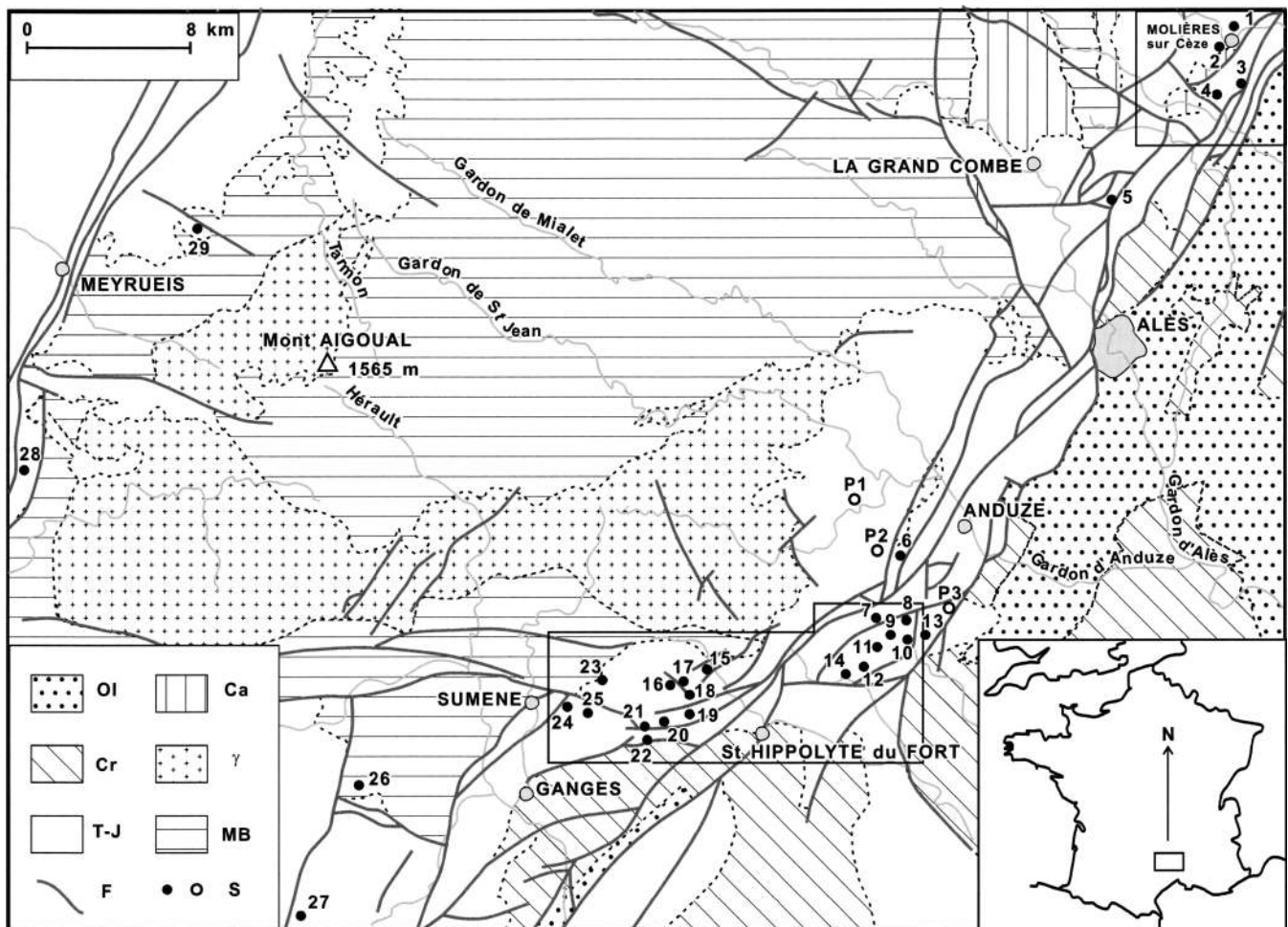

Figure 4. Cross-section presenting folding of the same bed in the Appalachian Mountains fold at Medley and at Rig: (a) present state (see text) and (b) during remagnetization. (c) Deformation, undergone after the remagnetization, of a plane which would have been horizontal during the remagnetization.

Figure 5. The Cévennes area and studied sites (S): Oligocene (Ol), Cretaceous (Cr) Triassic–Jurassic (T–J), Carboniferous (Ca), granites (γ), metamorphic basement (MB) and faults (F).

in southern France in order to date mineralization of Mississippi Valley-type (MVT). Results from a preliminary study indicated that magnetic overprint of about Eocene age affected a very large area (Rouvier *et al.* 1995), and thus the study was enlarged to include numerous sites in different parts of the Cévennes border (48 sites, 961 samples). All the samples were progressively demagnetized, allowing determination of characteristic remanent magnetization (ChRM). The fact that this ChRM is a remagnetization is clearly demonstrated at the La Grande Vernissière site. This site corresponds to a karst cavity, where part the roof collapsed before deposition of some detrital sediment and the filling of the cavity by carbonated matrix. The collapsed blocks have a chaotic orientation. We collected 83 samples within collapsed blocks as well as from the walls of the cavity, from the detrital sediments and from the carbonated matrix. The direction of the ChRM appears to be identical in all the samples in geographical coordinates. Bedding correction (using their initial stratification plane for the collapsed blocks) yields scattered ChRM directions (Fisher 1953, precision parameter *k* varying during this correction from 149 to 12,). The ChRM is therefore a remagnetization. Some of the 48 Cévennes sites were clearly affected by local rotation, and 15 sites (244 samples) were selected in areas that were certainly not affected by rotation. Using these sites, Henry *et al.* (2001) and Rouvier *et al.* (2001) determined the direction of the remagnetization ($D = 3.3°$, $I = 55.6°$, $k = 2155$ and

$\alpha_{95} = 0.8°$) and showed that the remagnetization is a syntectonic magnetic overprint of Lower to Middle Eocene age. Part of the present work on the Cévennes border is based on the palaeomagnetic data from the remaining 33 sites. The palaeomagnetic and rockmagnetic characteristics are very similar for all the sites studied in this area, and will not be described again here (see Henry *et al.* 2001; Rouvier *et al.* 2001, for these characteristics). To determine the direction of remagnetization in each site, at each resampling a small circle has been obtained with a bootstrap of the sample's palaeomagnetic direction. For the dip, a parametric bootstrap has been used for an uncertainty of 5° on the dip azimuth.

Fold

We sampled 10 of our sites (197 samples) along section across a large half-anticline cut by erosion in the southern flank of 'La Montagne de la Fage' (locations 16 to 22 on Fig. 5 and Table 2). Here again there is no evidence of superimposed folding with a fold axis of significantly different orientation. The southern part of this structure is cut by WSW–ENE faults. Table 2 gives the palaeomagnetic directions obtained and the present dip at these sites. The main fold is nearly cylindrical, with an almost horizontal fold axis. Such a nearly cylindrical fold should have given neighbouring small circles. However, the structure of the fold has been perturbed by local rotations (see next section) which are related to faults and which make the

Table 2. Palaeomagnetic results from the Montagne de la Fage anticline: site (number corresponds to location on Fig. 5); age of the formation (L.: Lower; U.: Upper); number of samples (*N*); azimuth (Az) and plunge value (Dip) of the mean present dip; dip value during remagnetization (Remag. dip)—a negative value indicates a dip towards an azimuth opposite to that of the present dip; declination (D), inclination (I) and Fisher (1953) parameters (*k*, *α*₉₅) at 0 per cent unfolding, 100 per cent unfolding and optimal unfolding from small circles analysis; rotation relative to stable sites (Rotation) determined using 'inclination' (1), with its uncertainty (+/−), and 'closest point' (2) methods.

Site	Age	N	Mean dip: present		Remag.	0 per cent unfolding				100 per cent unfolding				Optimal unfolding				Rotation (°)		
			Az (°)	Dip (°)	dip (°)	D (°)	I (°)	k	α₉₅(°)	D (°)	I (°)	k	α₉₅(°)	D (°)	I (°)	k	α₉₅(°)	1	±	2
16	L. Sinemurian	37	154.2	8.4	−5.0	1.4	44.2	191	1.7	6.4	51.3	156	1.8	9.3	55.7	578	1.0	+6.2	1.7	+4.2
16	U. Sinemurian	17	137.4	6.5	−12.6	9.0	43.0	240	2.2	14.3	46.8	255	2.1	24.9	55.7	31	6.1	+21.8	10.6	(+10.7)
17	L. Lotharingian	33	182.8	12.4	−2.8	4.2	40.5	516	1.1	4.9	52.9	477	1.1	4.7	55.7	809	0.9	+1.6	0.9	+1.7
17	U. Lotharingian	18	139.3	28.7	−7.6	359.5	21.9	247	2.1	13.0	41.3	293	1.9	(18.7)	(45.2)	472	1.5	–	–	(+15.6)
18	Carixian	25	159.3	38.8	−9.8	356.8	11.5	103	2.8	6.0	47.4	116	2.6	11.1	55.7	825	1.0	+9.9	0.8	(+7.0)
19	Domerian	8	160.0	42.8	−7.6	340.5	5.4	196	3.5	341.5	48.2	195	3.5	341.9	55.7	344	2.7	−21.2	2.5	−21.0
20	Toarcian	14	150.0	50.0	−4.8	316.3	1.7	322	2.1	351.0	51.0	322	2.1	352.2	55.7	908	1.2	−10.9	1.3	(−10.3)
21	Aalenian	13	163.5	50.6	−4.3	345.6	0.8	122	3.4	347.9	51.4	151	3.0	348.2	55.7	215	2.5	−14.9	2.3	−14.5
22	Bathonian	9	170.0	75.0	49.2	359.8	30.6	35	7.9	136.1	71.1	35	7.9	5.5	55.7	109	4.5	+2.4	5.1	+2.2
22	Portlandian	23	184.2	53.8	1.7	5.0	4.2	15	7.4	358.9	56.8	16	7.3	359.9	55.7	138	2.5	−5.4	2.5	−5.2
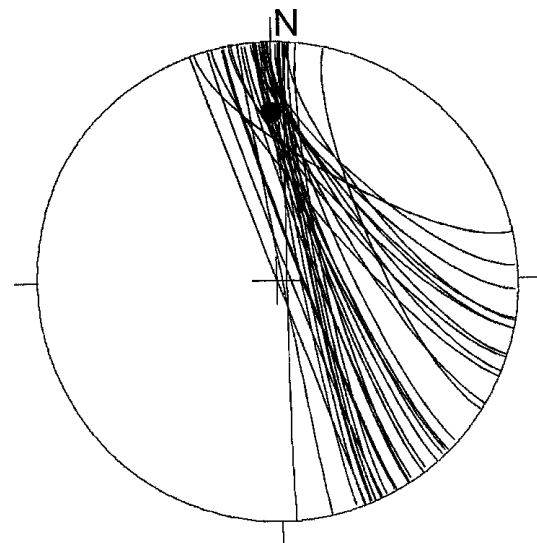
Figure 6. Small circles associated with the syntectonic remagnetization in the Montagne de la Fage section on the Cévennes border. The full circle indicates the remagnetization direction (Henry *et al.* 2001; Rouvier *et al.* 2001; Lewchuk *et al.* 2004). Stereographic projection in the lower hemisphere.

intersection of the small circles (Fig. 6) unreliable. Correction was made for the local rotations assuming a similar orientation of the fold axis at all the sites. The direction of remagnetization then becomes totally undetermined for this fold. However, contrary to the case of southern Virginia, this direction of the remagnetization (called until the end of this paper the 'reference direction') is already known here from other sites (Henry *et al.* 2001; Rouvier *et al.* 2001) and it is thus possible to calculate the dip for each site. The initial direction of the remagnetization and corresponding dip values at the sites of the Montagne de la Fage section are given in the Table 2. Figs 7(a) and (b) represent the shape of the fold for the same bed in its present state (Fig. 7a) and during remagnetization (Fig. 7b). Fig. 7(c) presents the
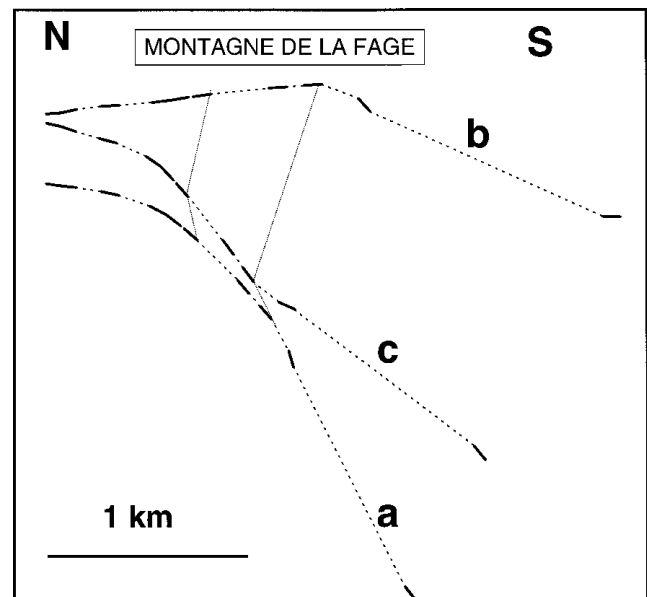
Figure 7. Cross-section presenting folding of the same bed in the Montagne de la Fage fold: (a) present state (see text) and (b) during remagnetization. (c) Deformation, undergone after the remagnetization, of a plane which would have been horizontal during the remagnetization.

present deformation of a plane which would have been horizontal during the remagnetization. Before magnetic overprinting, the mean dip of the series was mainly weak and northwards. In the southern part of the section, there was, however, a flexure just at the level of a present WSW–ENE fault. After the remagnetization, the deformation is marked by folding with a larger radius of curvature, which is related to the main Pyrenean tectonic phase in this area. This evolution—moderate folding and remagnetization followed by the main folding—is very similar to that pointed out in the Appalachian Mountains fold.

Local rotations

In some sites, the direction of remagnetization, known from other sites that were not affected by local rotations, is not very close to the small circle. This indicates that rotation with a strongly dipping axis affected this site. We have to bear in mind that the remagnetization is syntectonic, and therefore also involves the effects of folding. The method used to study the rotations is then based on determination of the part of the small circle possibly related to the direction of remagnetization; it consists of analysis of the inclination on the small circle (Waldhör 1999). The direction retained on the small circle is that with the same inclination as the direction of remagnetization that was determined in stable areas (the reference direction).

There are two possible main problems with this approach:

(1) In some cases with a fold axis and reference direction with neighbouring azimuths, all directions on the small circle have a lower inclination than the reference direction (for example, because of a late general tilting). To determine the retained direction, use of the direction with the highest inclination on the small circle would be meaningless because the azimuth of the direction with the highest inclination is related to the fold axis.

(2) The second problem is that for the other cases there are mostly two points on the small circle with the inclination of the reference direction. Sometimes, structural arguments alone enable the choice between these two points to be made.

To solve these two difficulties, another method of estimating the retained direction has been used. It consists of the determination by the least-squares method on the small circle of the direction closest to the reference direction. This direction can be retained as a possible direction of remagnetization only if the windows of inclination (inclination $\pm\alpha_{95}$ values) for this retained direction and for the reference direction overlap, at least in part. Comparison of the results obtained by this 'closest direction' and the 'inclination' methods shows that the calculated rotation relative to stable areas is always lower (or the same) when using the 'closest direction' approach. The rotation determined by the latter could therefore be underestimated and thus the 'inclination' method is more reliable. If all points on the small circle have lower inclinations than the reference direction, this 'closest point' approach is the only method that can be used. If two points are possible on the small circle using the 'inclination' method, the point nearest to the direction obtained by the 'closest direction' approach was chosen.

In addition to the 10 sites of La Montagne de la Fage, we studied 23 other sites (520 samples) in areas that could have been affected by rotations on the Cévennes border. These palaeomagnetic results are summarized in Table 3. Tables 2 and 3 also present the retained

Table 3. Palaeomagnetic results from the other Cévennes sites: site (number corresponds to location on Fig. 5); number of samples (*N*); age of the formation; azimuth (Az) and plunge value (Dip) of the mean present dip (between brackets for sites with moderate dip variation, no values for sites with significant dip variation); declination (D), inclination (I) and Fisher (1953) parameters (*k*, α_{95}) at 0 per cent unfolding, 100 per cent unfolding and optimal unfolding from small circles analysis; rotation relative to stable sites (Rotation) determined using 'inclination' (1), with its uncertainty (+/−), and 'closest point' (2) methods. For the Grande Vernissière data (site 11), the first line is based on the dip measured on the samples (collapsed blocks in a karstic cavity) and the second one on the dip corresponding to a tilting of the whole series. For La Gardie (site 26), the dip used is that from the overlying Mesozoic series.

Site	N	Age	Mean dip: present		0 per cent unfolding				100 per cent unfolding				Optimal unfolding				Rotation (°)		
			Az (o)	Dip (°)	D (°)	I (°)	k	α_{95}(°)	D (°)	I (°)	k	α_{95}(°)	D (°)	I (°)	k	α_{95}(°)	1	±	2
1	44	Hettangian	–	–	15.6	69.0	478	1.0	3.9	62.8	113	2.0	355.1	55.7	129	1.9	−8.0	2.4	(−3.8)
2	28	Hettangian	5	13	14.3	66.5	618	1.1	10.8	53.6	618	1.1	10.9	55.7	1773	0.6	+7.8	0.6	+7.8
3	33	Hettangian	(320)	(18)	10.3	60.8	396	1.2	354.5	48.1	374	1.3	1.0	55.7	402	1.2	−2.1	1.6	−1.0
4	11	Carixian	(276)	(22)	0.7	58.2	214	2.9	332.9	50.0	122	3.8	3.7	57.6	320	2.4	–	–	+.06
4	26	Hettangian	(322)	(18)	12.2	61.0	246	1.8	355.1	46.8	130	2.4	2.4	55.7	435	1.3	−0.7	1.7	−0.2
5	22	Triassic	(134)	(18)	22.1	51.0	73	3.5	47.5	51.7	56	4.0	(12.5)	(48.2)	126	2.7	–	–	(+9.1)
6	11	Triassic	–	–	26.6	52.5	324	2.3	60.4	62.7	324	2.3	31.7	55.7	637	1.7	+28.6	4.0	(+19.0)
7	8	Hettangian	280	41	66.5	31.0	221	3.3	33.4	60.0	221	3.3	(1.5)	(62.9)	295	2.9	–	–	(−1.6)
8	12	Hettangian	100	18	15.4	59.5	220	2.7	40.2	53.1	220	2.7	(2.3)	(59.6)	272	2.5	–	–	(−0.8)
9	34	Sinemurian	(143)	(21)	8.1	45.0	249	1.5	31.1	56.9	132	2.1	(14.1)	(50.0)	389	1.2	–	–	(+11.0)
10	28	Sinemurian	–	–	4.7	52.3	192	1.9	15.8	52.7	70	3.2	(5.4)	(52.1)	515	1.2	–	–	(+2.1)
11	83	Sinemurian	–	–	27.7	50.1	149	1.3	40.1	37.2	12	4.5	–	–	–	–	–	–	–
	83		235	10	27.7	50.1	149	1.3	20.5	58.7	149	1.3	23.6	55.7	362	0.8	+20.3	1.3	(+14.2)
12	14	Carixian	220	12	22.5	41.9	417	1.8	18.4	53.4	417	1.8	16.9	55.7	772	1.3	+13.6	1.7	(+11.9)
13	11	Toarcian	0	0	18.1	49.4	85	4.6	18.1	49.4	85	4.6	19.9	53.8	139	3.6	–	–	+16.8
14	17	Toarcian	(160)	(31)	6.0	29.8	111	3.2	23.4	55.1	70	4.1	23.4	55.7	262	2.1	+20.3	4.0	(+14.7)
15	22	Hettangian	(210)	(21)	357.3	45.4	521	1.3	339.0	61.0	583	1.2	347.7	55.7	995	0.9	−15.1	2.6	(−11.5)
23	12	Triassic	150	20	8.9	49.7	261	2.5	32.8	62.2	261	2.5	16.1	55.7	779	1.4	+13.0	3.9	(+8.4)
24	21	Hettangian	(205)	(29)	21.9	34.9	269	1.9	19.9	63.0	140	2.6	23.3	55.7	258	1.5	+20.2	4.5	+18.0
25	15	Toarcian	(170)	(39)	11.8	26.0	179	2.7	32.8	59.3	179	2.7	27.3	55.7	262	2.2	+24.2	3.8	(+19.7)
26	17	Cambrian	195	10	5.9	49.4	25	6.8	3.4	59.3	25	6.8	4.9	55.7	48	4.9	+1.6	4.5	+1.6
27	17	Hettangian	(80)	(6)	19.3	57.2	229	2.2	26.9	53.5	208	2.4	(6.5)	(60.7)	343	1.8	–	–	(+3.4)
28	28	Sinemurian–Lotharingian	–	–	5.9	65.9	70	3.2	2.2	50.5	54	3.6	6.1	55.7	60	3.4	+3.0	7.9	−1.4
29	16	Hettangian	–	–	7.3	57.0	136	3.0	1.0	53.1	21	7.7	7.0	55.7	250	2.2	+3.9	2.9	2.7
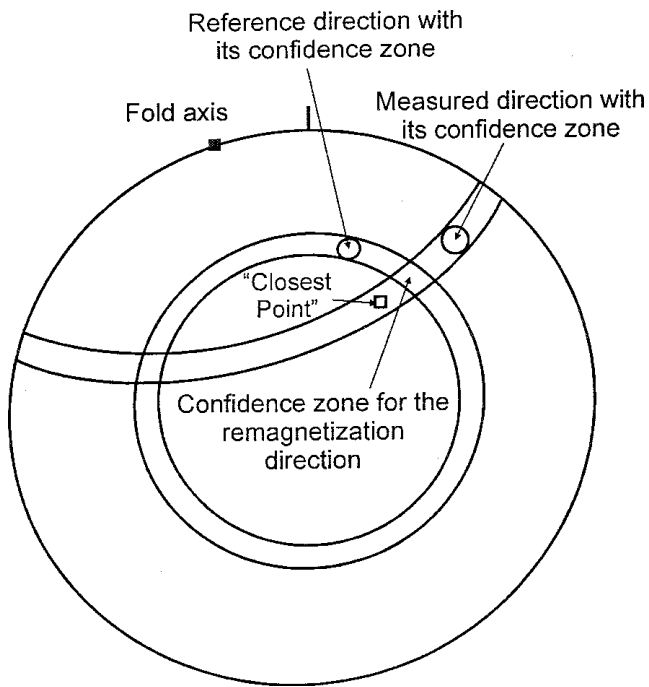
Figure 8. Graphical determination of the confidence region. Stereographic projection in the lower hemisphere. Possible orientations of the reference direction (with its confidence zone) in the area affected by rotation with vertical axis corresponds to all directions with the same inclination (on the figure, area between the two circles with vertical axis). Possible initial orientations of the measured direction (with its confidence zone) in a fold corresponds on the figure to all directions between the two circles with horizontal axis. See text for details.

direction of remagnetization and the rotation angle undergone by the sites relative to stable areas that were deduced by using both methods in the Cévennes area. Values between brackets are those determined by the 'closest direction' method, but associated with windows of inclination corresponding to the confidence regions for the retained direction and for the reference direction that do not at least partially overlap. Results obtained by Kechra *et al.* (2003) in the same area mainly correspond to rotated sites and they yield similar rotations.

For determination of uncertainty on rotation, confidence regions have to be corrected (Demarest 1983). Uncertainty about the retained direction can be estimated by a graphical method using the corrected confidence regions of both the retained and reference directions (Fig. 8). The larger uncertainty for rotation relative to that for a simple fold is merely due to the fact that both rotation and fold occurred. Tables 2 and 3 include the uncertainty values.

The main tectonic structure on the eastern border of the Cévennes is the northeast–southwest Cévennes fault region. This structure, of Hercynian age, underwent important sinistral movement during Pyrenean north–south compression. Some of our sampling sites (Fig. 5) were concentrated in this fault zone. We also studied several sites, including the Montagne de la Fage section, west of these northeast–southwest Cévennes faults and north of the eastern extensions of the Alzon Fault, that trend mainly WNW–ESE,. Finally, four sites were chosen on the southern and western borders of the Cévennes.

In the general context of the sinistral Cévennes shear zone, counter-clockwise rotations were expected. However, no coherent rotation has been revealed along the zone of the Cévennes fault (Fig. 9 and Table 3) . The moderate clockwise and counter-clockwise rotations obtained could be the effect of very local deformation close to the fault. The lack of coherent rotation in this shear zone could be explained by the very elongated shape of the blocks delimited by northeast–southwest faults. No significant rotations have been obtained for the southern and western border of the Cévennes either. Surprisingly however, (Fig. 9 and Tables 2 and 3), clockwise rotations, which are sometimes very important (exceeding 20°), have been found throughout the studied area north of the eastern extensions of the Alzon Fault, except for few sites showing an counter-clockwise rotation. This area is characterized by the presence of different structural directions: mainly those of the Cévennes faults trending northeast–southwest and the WNW–ESE direction of the Alzon Fault. But numerous faults here are curved. These faults delimit structural blocks, which are much less elongated than along the Cévennes faults, often with such curved borders. In this area, which is close to the stable basement of the Massif Central, rotation of a very large block is not a realistic assumption. The observed counter-clockwise rotations (Le Mazet (site 15), middle and southern parts of the Montagne de la Fage section) are all for sites lying very close to faults. On the contrary, no evidence of faults has been found close to the other sites with clockwise rotations. This suggests that this area mainly corresponds to small blocks which underwent clockwise movements. The faults had sinistral movements along their border, which produced the local counter-clockwise rotations that were observed. This area shows therefore a typical Riedel structure (Riedel 1929; Boudon *et al.* 1976). In addition to the sinistral displacement along the Cévennes fault, shortening related to the north–south Pyrenean compression was considered to be mainly restricted to a few reverse faults and to the local east–west axis folding in the Cévennes border. We know now that it was also locally accommodated by small block rotation.

CONCLUSION

The analysis of syntectonic remagnetizations represents a strong tool for structural studies that gives access to information which cannot be obtained by other methods. In the fold studied in the Cévennes border, the magnetic overprinting occurred relatively early during the deformation. However, examples of remagnetization acquired in various stages of folding in the same area have been also observed (Villalain *et al.* 1994, 1996), and sometimes related to diachronic evolution of the folds according to their structural position (Stamatakos & Hirt 1994; Jordanova *et al.* 2001). The case of local rotations is not so easily constrained because, in practice, the movement undergone involves both rotation and folding. However, in the Cévennes area, analysis of the syntectonic remagnetization reveals strong rotations that are not brought to light by classical structural analyses.

ACKNOWLEDGMENTS
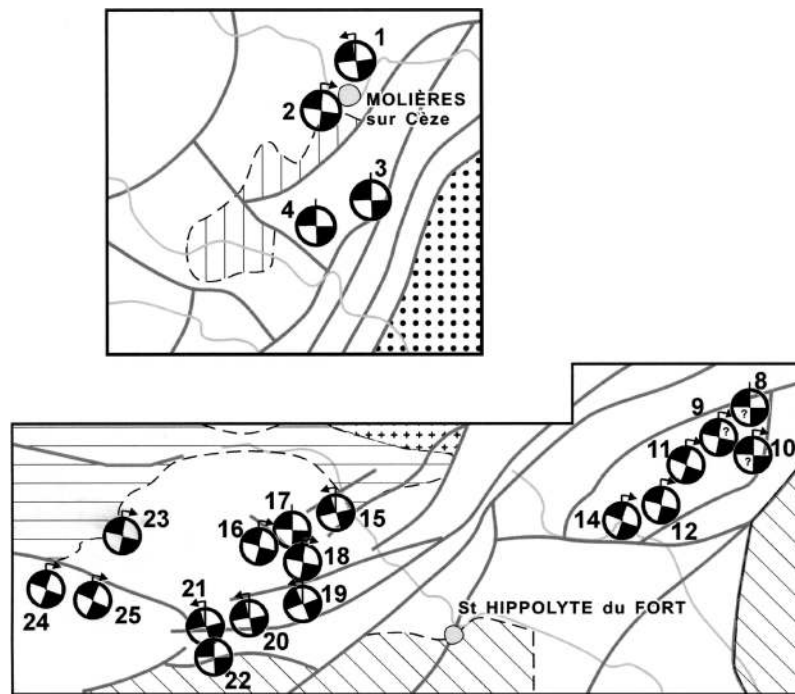
Figure 9. Rotation in sites 1 to 4 near Molières sur Cèze and in sites 11 to 25 around Saint Hippolyte du Fort. For each site the arrow indicates the direction of rotation and the angle of rotation is shown by the symbol.

REFERENCES

Bazhenov, M.L. & Shipunov, S.V., 1991. Fold test in paleomagnetism: new approaches and reappraisal of data, *Earth planet. Sci. Lett.,* **104,** 16–24.

Boudon, J., Gamond, J.F., Gratier, J.P., Robert, J.P., Depardon, J.P., Gay, M., Ruhland, M. & Vialon, P., 1976. L'arc alpin occidental: réorientation de structures primitivement E–W par glissement et étirement dans un système de compression global N–S?, *Eclogae geol. Helv.,* **69,** 509–519.

Constable, C. & Tauxe, L., 1990. The bootstrap for magnetic susceptibility tensors., *J. geophys. Res.,* **95,** 8383–8395.

Demarest, H.H., 1983. Error analysis for the determination of tectonic rotation from paleomagnetic data, *J. geophys. Res.,* **88,** 4321–4328.

Derder, M.E.M., Henry, B, Bayou, B., Djellit, H. & Amenna, M., 2001. New Moscovian paleomagnetic pole from the Edjeleh fold (Saharan craton, Algeria), *Geophys. J. Int.,* **147,** 343–355.

Efron, B., 1982. *The Jackknife, the Bootstrap, and Other Resampling Plans,* CBMS-NSF Regional Conference Series in Applied Mathematics Vol. 38, SIAM, Philadelphia, PA.

Efron, B. & Tibshirani, R., 1986. Bootstrap methods for standard errors, confidence intervals, and other measures of statistical accuracy. *Stat. Sci.,* **I,** 54–77.

Enkin, R.J. & Watson, G.S., 1996. Statistical analysis of paleomagnetic inclination data, *Geophys. J. Int.,* **126,** 495–504.

Fisher, N.I. & Hall, P., 1990. New statistical methods for directional data -I. Bootstrap comparison of mean directions and the fold test in palaeomagnetism, *Geophys. J. Int.,* **101,** 305–313.

Fisher, N.I. & Hall, P., 1991. A general statistical test for the effect of folding, *Geophys. J. Int.,* **105,** 419–427.

Fisher, R.A., 1953. Dispersion on a sphere, *Proc. R. Soc. Lond.,* A, **217,** 295–305.

Henry, B., 1983. *Corrections Structurales Indispensables pour le Paléomagnétisme en Zone Déformée*, publication CRE 83/05, Laboratoire Tectonophysique, Paris.

Henry, B., 1997a. The magnetic zone axis: a new element of magnetic fabric for the interpretation of the magnetic lineation, *Tectonophysics,* **271,** 325– 331.

Henry, B., 1997b. Bootstrap and magnetic fabric, *EUG 9 Meeting, Strasbourg*.

Henry, B., 1999. Confidence zone from remagnetization circles: a new possibility for the fold tests, *EUG 10 Meeting, Strasbourg*.

Henry, B. & Le Goff, M., 1994. A new tool for paleomagnetic interpretation: the bivariate extension of the Fisher statistics. *XIX EGS General Assembly, Grenoble*.

Henry, B, Becq-Giraudon, J.F. & Rouvier, H., 1999. Paleomagnetic studies in the Permian basin of Largentière and implications for the Late Variscan rotations in the French Massif Central, *Geophys. J. Int.,* **138,** 1888–1898.

Henry, B, Rouvier, H., Le Goff, M., Macquar, J.C., Thibiéroz, J., Lewchuk, M.T. & Leach, D., 2001. Paleomagnetic dating of the widespread remagnetization on the southeastern border of the French Massif Central and implications for fluid flow and MVT mineralization, *Geophys. J. Int.,* **145,** 368–380.

Jordanova, N., Henry, B., Jordanova, D., Ivanov, Z., Dimov, D. & Bergerat, F., 2001. Paleomagnetism in north-western Bulgaria: geological implications of widespread remagnetization, *Tectonophysics,* **343,** 79– 92.

Kechra, F., Vandamme, D. & Rochette, P., 2003. Tertiary remagnetization of normal polarity in Mesozoic marly limestones from SE France, *Tectonophysics,* **362,** 219–238.

Lewchuk, M.T., Elmore, D. & Evans, M., 2002. Remagnetization signature of Paleozoic sediments from the Patterson Creek anticline in West Virginia, *Phys. Chem. Earth,* **27,** 1141–1150.

Lewchuk, M.T., Rouvier, H., Leach, D., Henry, B., Le Goff, M., Macquar, J.C. & Thibiéroz, J., 2004. Paleomagnetism of Mississippi Valley-type (MVT) mineralization in the southern border of the French Massif Central and its relationship to Pyrénées orogenesis, *Miner. Deposita*. Submitted.

McClelland-Brown, E., 1983. Palaeomagnetic studies of fold development and propagation in the Pembrokeshire old red sandstone, *Tectonophysics,* **98,** 131–149.

McElhinny, M.W., 1964. Statistical significance of the fold test in palaeomagnetism, *Geophys. J. Roy. astr. Soc.,* **8,** 338–340.

McFadden, P.L., 1990. A new fold test for palaeomagnetic studies, *Geophys. J. Int.,* **103,** 163–169.

McFadden, P.L. & Jones, D.L., 1981. The fold test in palaeomagnetism, *Geophys. J. R. Astr. Soc.,* **67,** 53–58.

McFadden, P.L. & McElhinny, M.W., 1988. The combined analysis of remagnetization circles and direct observations in palaeomagnetism, *Earth planet. Sci. Lett.,* **87,** 161–172.

Riedel, W., 1929. Zur Mechanik geologischer Brucherscheinungen, *Zentralblatt Mineral. Geol. Palaeontol.,* B, 354–368.

Rouvier, H., Henry, B. & Le Goff, M., 1995. Regional remagnetization and Mesozoic levels containing 'Mississippi Valley type' deposits: the southern border of the French Massif Central, *XXIth IUGG General Assembly, Boulder.*

Rouvier, H., Henry, B., Macquar, J.C., Leach, D., Le Goff, M., Thibiéroz, J. & Lewchuk, M.T., 2001. Réaimantation régionale éocène, migration de fluides et minéralisations dans la bordure cévenole, *Bull. Soc. Géol. Fr.,* **172,** 503–516.

Shipunov, S.V., 1997. Synfolding magnetization: detection testing and geological applications, *Geophys. J. Int.,* **130,** 405–410.

Stamatakos, J. & Hirt, A.M., 1994. Paleomagnetic considerations of the development of the Pennsylvania salient in the central Appalachians, *Tectonophysics,* **231,** 237–255.

Surmont, J., Nikolov, T, Thierry, J., Peybernes, B. & Sapunov, I., 1991. Paléomagnétisme des formations sédimentaires jurassiques et éocrétacées des zones de Stara Planina-Prébalkan et de Luda Kameija (Balkanides externes, Bulgarie), *Bull. Soc. Géol. Fr.,* **162,** 57–68.

Tauxe, L. & Watson, G.S., 1994. The fold test: an eigen analysis approach., *Earth planet. Sci. Lett.,* **122,** 331–341.

Tauxe, L., Kylstra, N. & Constable, C., 1991. Bootstrap statistics for paleomagnetic data, *J. geophys. Res.,* **96,** 11 723–11 740.

Villalain, J.J., Osete, M.L., Vegas, R., Garcia-Duenas, V. & Heller, F., 1994. Widespread Neogene remagnetization in Jurassic limestones of the south-Iberian palaeomargin (western Betics, Gibraltar Arc), *Phys. Earth planet. Inter.,* **85,** 15–33.

Villalain, J.J., Osete, M.L., Vegas, R., Garcia-Duenas, V. & Heller, F., 1996. The Neogene remagnetization in the western Betics: a brief comment on the reliability of palaeomagnetic directions. In *Palaeomagnetism and Tectonics of the Mediterranean Region*, Geological Society Special Publication 105, pp. 33–41, eds Morris A. & Tarling D.H., Geological Society, London.

Waldhör, M., 1999. The small circle reconstruction in palaeomagnetism and its application to palaeomagnetic data from Pamir, *Thesis,* Tübingen.

Watson, G.S. & Enkin, R.J., 1993. The fold test in paleomagnetism as a parameter estimation problem, *Geophys. Res. Lett.,* **20,** 2135–2137.